

Fuel and time minimization in a CVT wheel loader application

Tomas Nilsson* Anders Fröberg** Jan Åslund***

* Department of Electrical Engineering, Linköping University,
Linköping, Sweden, (email: tnilsson@isy.liu.se)

** Volvo CE, Eskilstuna, Sweden, (email: anders.froberg@volvo.com)

*** Department of Electrical Engineering, Linköping University,
Linköping, Sweden, (email: jaasl@isy.liu.se)

Abstract: A method is developed for the minimization of time and fuel required for performing a short loading cycle with a CVT wheel loader. A factor β is used for weighing time to fuel in the optimization. Dynamic programming is used as optimization algorithm, and the developed method is based on the change of independent variable, from time to distance driven. It is shown that a change of states from speeds to kinetic energies in the internal simulations is essential. A driving cycle, derived from measurements, representing a short loading cycle is introduced. Optimization is performed against this cycle according to the method presented, using two different values on the time to fuel weighing parameter. It is shown that this parameter can be used to find optimal solutions directed toward short time or low fuel consumption.

Keywords: Vehicles, Wheel loaders, Continuously variable transmission, Optimization, Dynamic programming, Simulation

1. INTRODUCTION

1.1 Background

The common wheel loader operation is characterized by its highly transient nature and periods of high tractive effort at low speed. The engine also delivers power both to the transmission and to the working hydraulics pump. The most common general transmission layout of heavy wheel loaders is presented in Figure 1. The engine is connected to the transmission and a variable-displacement working hydraulics pump. In present machines the transmission is usually of a torque converter and automatic gearbox type. This type of transmission is well suited for the typical operation, but in some modes of operation the efficiency is low. Since the efficiency drawbacks are highly related to the use of a torque converter, there is a desire to find other transmission concepts for wheel loaders.

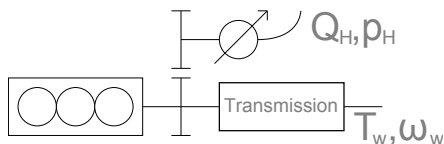


Fig. 1. General wheel loader drivetrain setup.

One alternative to the present setup is infinitely variable transmissions, such as the electric used in Filla (2008) or the hydrostatic used in Rydberg (1998). The drawback with this type of transmission is that the repeated power conversions reduce the efficiency. Power-split devices such as those used in Carl et al. (2006) and Grammatico et al. (2010) has two or more parallel power paths, allowing for increased efficiency. Multi-mode CVTs are constructed so

that several power-split layouts can be realized with the same device, enabling high efficiency at widely spaced gear ratios. In this paper, just as in Savaresi et al. (2004), a hydrostatic multi-mode CVT concept is analyzed.

1.2 Optimal control

When the torque converter is replaced with a less flexible component the demand for active control increases, see for example Zhang (2002). The quality of the control is also critical for the successful implementation of the concept. Optimization methods can be used to find the minimal cost and the corresponding control trajectories for performing a desired task. This has for example been done in Pfiffner and Guzzella (2001), Sivertsson and Eriksson (2012) and Murgovski (2012). In Hellström (2010) predictive control is used in a feedback application for realizing a fuel consumption near the minimum. This type of operation rely on having a prediction of future load. Wheel loaders commonly operate in highly repetitive patterns, such as the short loading cycle described in Filla (2005), which may form the basis for such a prediction. Lack of prediction accuracy was treated in Nilsson et al. (2012a) by the introduction of a statistical loading cycle and stochastic optimization. Still, the strict time dependency in the load cases and optimization may restrict the optimizer. Introducing a freedom in time, just as in Hellström et al. (2010), may allow for lower fuel consumption while reducing sensitivity to prediction uncertainties. Because of the complexity of the wheel loader vehicle and operation this paper focus on investigating the implementation of a combined minimization of fuel and time and consider disturbances only in bucket load weight prediction.

2. PROBLEM FORMULATION

The general layout of the system is presented in the introduction, in Figure 1. In the vehicle presented here, the standard transmission is replaced with a CVT, but no other changes are made. The following sections formalize the problem and present the models for each of the system components.

2.1 Problem statement

The problem considered in this paper is the minimization of total amount of fuel M_f and time T for performing a short loading cycle. The factor β is introduced to weigh time to fuel in the minimization. This can be expressed as

$$\min \{M_f + \beta T\} \quad (1)$$

Optimization is performed for a number of different β . This analysis is extended with an analysis of the sensitivity to disturbances in the weight of the load in the bucket.

2.2 Load cases

In this work the input from the driver is interpreted as a desired bucket trajectory. This desired trajectory must be exactly followed, as fast as possible and using as little fuel as possible. Since a freedom in time is introduced, the load is expressed as a function of position. The bucket trajectory can then be expressed as bucket height as a function of distance driven. This height is expressed as the corresponding volume in the lifting hydraulic cylinders.

The external forces that act on the vehicle, assuming flat ground and low speeds, are the rolling resistance and the vertical and longitudinal forces on the bucket. The vertical bucket-force can be expressed as a pressure in the working hydraulic system and the longitudinal bucket-force can be lumped with the rolling resistance. The forces acting on the bucket has a complicated dependency on the bucket trajectory, the weight of the load, the type of material handled and the shape of the pile from which material is collected, see Filla (2008). Optimization is therefore only performed against trajectories and corresponding forces derived from measurements. It is assumed that the load forces are independent of the bucket speed.

Since the machine drives in reverse direction part of the time, the velocity v_w is divided into speed $v_s = |v_w|$ and direction $d_s = \text{sign}v_w$. The driving cycle therefore consist of hydraulic volume V_H , hydraulic pressure p_H , rolling resistance F_w and direction of driving d_s , as functions of distance driven $s = \int v_s dt$.

2.3 Vehicle model

The vehicle is modeled as a mass m for which the speed dynamics depend on the tractive torque T_W , the brake torque T_b and the resistance force F_w . The vehicle mass is the sum of the mass of the empty vehicle m_v and the bucket load m_L , and the resistance force is the sum of rolling resistance $c_r mg$ and longitudinal bucket force F_{BL} . The factor r is a gear ratio which includes the wheel radius.

$$\frac{dv_w}{dt} \cdot m = r^{-1}T_W - r^{-1}T_b - F_w \quad (2)$$

2.4 Engine model

The engine is modeled as an inertia I_e which is affected by the engine torque T_e , the transmission torque T_T and the hydraulic pump torque T_H .

$$\frac{d\omega_e}{dt} \cdot I_e = T_e - T_T - T_H \quad (3)$$

The relation between injected fuel and engine torque is described by a quadratic Willan's model, as presented in Rizzoni et al. (1999), expanded with a turbo model.

$$T_e = e(\omega_e, m_f) \cdot \frac{q_{lhv} n_{cyl}}{2\pi n_r} \cdot m_f - T_L(\omega_e) - T_{pt} \quad (4)$$

Here m_f is fuel mass per injection, ω_e is engine speed, e and T_L are efficiency functions. T_{pt} is torque loss due to lack of air intake pressure $p_{off} = p_t - p_{set}(\omega_e, m_f)$ caused by low turbo charger speed. The actual pressure is p_t and p_{set} is a static setpoint map. The turbo is modeled as a first order delay for the intake air pressure

$$\frac{dp_t}{dt} \cdot \tau(\omega_e) = -p_{off}(\omega_e, m_f) \quad (5)$$

The torque loss from low intake pressure is described by

$$T_{pt} = \begin{cases} k_1(\omega_e) \cdot p_{off}^2 - k_2(\omega_e) \cdot p_{off} & \text{if } p_{off} < 0 \\ 0 & \text{if } p_{off} \geq 0 \end{cases} \quad (6)$$

The fuel flow and fuel mass per injection are related according to

$$\frac{dM_f}{dt} = \omega_e \frac{n_{cyl}}{4\pi} m_f \quad (7)$$

Figure 2 presents the efficiency map of the engine used. The gray lines indicate the allowed operating region (minimum speed and maximum torque) and the black line indicates the static optimal operating points as a function of output power. The figure also shows efficiency levels and output power lines with kW markings.

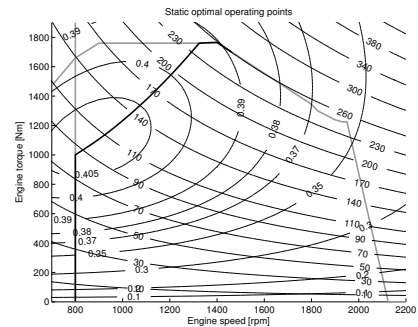


Fig. 2. Engine map with static optimal operation line, speed and torque limits, efficiency curves and output power lines with kW markings.

2.5 Multi-mode CVT model

The transmission used is the three mode forward/reverse ($m_T \in \pm[1, 2, 3]$) CVT described in the patent Mattsson and Åkerblom (2012), and has a structure similar to devices used in Savaresi et al. (2004) and Lauinger et al. (2007). The layout is presented in Figure 3, with the dark gray box representing a Ravigneaux planetary gearset and the light gray box representing a regular planetary gearset. The CVT functionality is provided by the two hydraulic

machines $H1$ & $H2$, which together form a 'variator'. Changing gear ratio within a mode is done by altering the ratio of the displacement of the hydraulic machines. The mode is selected by applying the corresponding clutch 1, 2 or 3. Mode shifts are performed at the extremals of the variator displacement, and mode shifts at these points do not change the overall gear ratio. At mode shifts the speed differences over the involved clutches are close to zero, and therefore clutch losses may be neglected. The transmission torques at the engine side T_T and the wheel side T_W of the transmission depend on the transmission mode m_T , the variator displacement ratio ψ_1 and the speeds ω_e and $r^{-1}v_s$. The complete functions $T_T(m_T, \psi_1, \omega_e, v_s)$ and $T_W(m_T, \psi_1, \omega_e, v_s)$ are omitted in this paper.

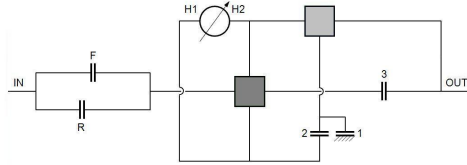


Fig. 3. Multi-mode CVT transmission layout.

The main source of losses in this concept is the variator, which is modeled according to the Equations (8) and (9). This model is based on Lennevi (1995).

$$\psi_1 D_v \omega_1 \pm p_v (C_a + (\omega_1 + \omega_2) C_b) - \psi_2 D_v \omega_2 = 0 \quad (8)$$

$$\psi_n D_v p_v - T_n \pm (C_c \omega_n + C_d p_v) = 0 \quad (9)$$

The index $n = 1, 2$ denotes the two machines, D_v is maximum displacement, $\psi \in (0, 1)$ is relative displacement, ω is axle speed, p_v is variator hydraulic pressure, T is torque and C_a, C_b, C_c and C_d are efficiency parameters. The signs in the equations depends on the power flow direction. Equation (8) describes hydraulic fluid flow and Equation (9) describes torque at each machine. The variator is constructed so that $\psi_1 + \psi_2 = 1$.

2.6 Hydraulics model

The bucket and boom are hydraulically operated. Pressure and flow of the hydraulic fluid is supplied by a variable displacement hydraulic pump connected to the engine. Equations (10) and (11) describe this pump.

$$q_H = \psi_H D_H \omega_e \quad (10)$$

$$q_H p_H = \eta_H T_H \omega_e \quad (11)$$

D_H is maximum displacement, $\psi_H \in [0, 1]$ is relative displacement and η_H is pump efficiency. In the sensitivity analysis, it is assumed that the pressure p_H is a linear function of the bucket load m_L .

3. METHOD

3.1 Loadcases

Wheel loader usage can often be described in a cycle framework. One of the most common cycles is the short gravel loading cycle. This cycle consists of moving forward and filling the bucket, reversing, moving forward towards a receiver and emptying the bucket, and finally reversing to the starting point. In a typical short loading cycle,

each movement can be around $10m$ and have a duration of around $5s$ with an additional $5s$ for the filling of the bucket, making a total of around $40m$ and $25s$ in a cycle. Measurements have been performed on a loader during a short loading cycle, and is used as an example in this paper. The driving cycle component V_H is calculated from the arm and bucket angles, the components p_H and d_s are measured and the component F_w is calculated from the torque converter input and output speeds for the bucket filling episode, and is assumed to be zero during the rest of the cycle. The bucket is assumed to be empty ($m_L = 0$) during the first and last episode and loaded in the other two. The masses are assumed to be $m_v = 26000kg$ and $m_L = 10000kg$ when loaded, in the $J(k, x)$ calculation. The complete load case used is displayed in Figure 4.

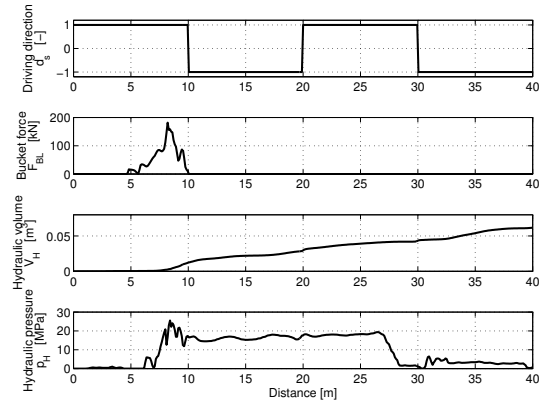


Fig. 4. The loadcase used is a short gravel loading cycle expressed by the components d_s , F_{BL} , V_H and p_H .

3.2 Change of independent variable

By reformulating the cost function and system dynamics to depend on distance driven ($s = \int v_s dt$) rather than time, a freedom in velocity can be introduced without the need to have time as a state of the system. The dynamics for a state x is rewritten, using the chain rule, according to

$$\frac{dx}{dt} = \frac{dx}{ds} \frac{ds}{dt} = \frac{dx}{ds} v_s = f(x(s), u(s), w(s)) \Rightarrow \quad (12)$$

$$\frac{dx}{ds} = \frac{1}{v_s} f(x(s), u(s), w(s)) \quad (13)$$

During the general driving cycle, the vehicle changes driving direction several times. At these instances the vehicle speed v_s has to go to zero. The state derivatives will then, according to the formulation (13), not be well defined. This is solved in different ways for the three states (v_s , ω_e and p_t) of the system. For the vehicle speed dynamics this can be solved by changing the state from speed to kinetic energy, using $m = m_v + m_L$, according to

$$\frac{d}{ds} \frac{m v_s^2}{2} = (r^{-1} T_W - r^{-1} T_b - F_w) \quad (14)$$

This solution is not available for the engine speed and turbo pressure dynamics though. Here the approximation

$$\Delta s = \bar{v}_s \Delta t, \quad \bar{v}_s = \frac{v_{s,k} + v_{s,k+1}}{2} \quad (15)$$

is instead used when the initial vehicle speed is close to zero. In the engine dynamics this approximation has to be supplemented with a correction of T_T to assure that the

transmission efficiency is not pushed to above 100% by the freedom in Δt . In these cases a constant transmission efficiency of $\alpha = 0.8$ is used. The components of the cost function (1) is rewritten according to

$$M_f = \int_0^{S_f} \frac{dM_f}{dt} dt = \int_0^{S_f} \frac{dM_f}{dt} \frac{ds}{v_s} \quad (16)$$

$$T = \int_0^{S_f} \frac{ds}{v_s} \quad (17)$$

which give the reformulated minimization criterion

$$\min \int_0^{S_f} \left(\frac{dM_f}{dt} + \beta \right) \frac{ds}{v_s} \quad (18)$$

3.3 Dynamic programming

Denote the applied load w and the discretized states $x \in X$, controls $u \in U$ and distance s_k with $k = 0, 1, \dots, N$. The optimization problem can then be stated as

$$\min_{u \in U} \left(J_N(x_N) + \sum_{k=0}^{N-1} g(x_k, u_k, w_k) \right) \quad (19)$$

along with system constraints. The deterministic dynamic programming (DDP) algorithm, which is described in detail in Bellman (1957); Bertsekas (2005), that recursively solves this problem can be formulated as

$$J_k(x_k) = \min_{u \in U} \left(g(x_k, u_k, w_k) + \tilde{J}_{k+1}(x_{k+1}(x_k, u_k, w_k)) \right) \quad (20)$$

in which \tilde{J}_{k+1} is found by interpolating over J_{k+1} . In the solution algorithm, the map $J(k, x)$ is first calculated. This map is then used in a one step look-ahead simulation to find the optimal state and control trajectories. The impact of prediction uncertainties can be analyzed by using different loads in calculating $J(k, x)$ and in the subsequent simulation. The algorithm, as applied here, is described in detail in Nilsson et al. (2011, 2012b). This method is well known, straight-forward, does not require an initial guess and guarantees global optimum. The drawback is that the number of simulations and interpolations grows rapidly with the number of states and controls and the corresponding discretization densities.

The controls available are the fuel mass per injection m_f , the variator displacement ratio ψ_1 , the transmission mode M_T and the brake torque T_b . The states of the system are the vehicle speed v_s , the engine speed ω_e and the turbo pressure p_t . The terminal cost $J_N = 0$ is used and the cost function, as defined in (18), is

$$g(x_k, u_k, w_k) = \left(\frac{dM_f}{dt} + \beta \right) \Delta t \quad (21)$$

in which the time steps $\Delta t = \Delta s/v_{s,k}$ or, if $v_{s,k} \approx 0$, $\Delta t = 2\Delta s/(v_{s,k} + v_{s,k+1})$, are used.

The gain from the variator ratio ψ_1 to the torques T_T and T_W , according to the functions $T_T(m_T, \psi_1, \omega_e, v_s)$ and $T_W(m_T, \psi_1, \omega_e, v_s)$, is very high. A high density ψ_1 control signal grid must therefore be used. This would however have a severe effect on the calculation effort. For this reason, a ψ_1 with high grid density but a narrow range centered around $\psi_1(m_T, \omega_e, v_s)$ s.t. $T_T(m_T, \psi_1, \omega_e, v_s) = 0$, is used.

3.4 Simulations and energy balance

The choice of dynamic programming for optimization method, combined with the complexity of the system, makes efficient simulation of the functions $x_{k+1}(x_k, u_k, w_k)$ decisive. The Euler forward method is the simplest method for this simulation, and using this method is therefore desirable. Direct application of this method on the aforementioned states however does not preserve energy. In fact, using the speed dynamics as an example, the Euler step is

$$v_{s,k+1} = v_{s,k} + \frac{\Delta s}{v_{s,k}} \frac{F}{m} \quad (22)$$

During this step the work performed by the force is

$$W_1 = F \Delta s \quad (23)$$

while the change in kinetic energy is

$$W_2 = \Delta \frac{mv_s^2}{2} = \frac{m}{2} (v_{s,k+1}^2 - v_{s,k}^2) = F \Delta s + \frac{1}{2m} \left(\frac{F \Delta s}{v_{s,k}} \right)^2 \quad (24)$$

and correspondingly for the rotational speed dynamics of the engine. There is obviously a discrepancy between the input and output energy. Since optimization algorithms uses shortcuts if there are any, this discrepancy will be exploited by pushing energy back and forth between the vehicle speed and engine speed. similar behaviour has been seen in e.g. Hellström et al. (2010) as solutions with oscillating control signals. In this system the gain from the control signal ψ_1 to the torques T_T and T_W is very strong, and the optimizer will therefore be highly inclined to using this shortcut. This problem can be prevented by using an energy formulation for both vehicle and engine speed dynamics, according to

$$\frac{d}{ds} \frac{mv_s^2}{2} = (r^{-1}T_W - r^{-1}T_b - F_w) \quad (25)$$

$$\frac{d}{dt} \frac{I_e \omega_e^2}{2} = \omega_e (T_e - T_T - T_H) \quad (26)$$

not only at low vehicle speeds. The Euler method simulation steps then become

$$v_{s,k+1} = \sqrt{v_{s,k}^2 + \frac{\Delta s}{m} \Sigma F} \quad (27)$$

$$\omega_{e,k+1} = \sqrt{\omega_{e,k}^2 + \frac{v_{s,k} \Delta t}{I_e} \Sigma T} \quad (28)$$

which guarantee the balance of energy.

4. EVALUATION

The developed weighted optimization is evaluated using the load case described in Section 3.1 and Figure 4. Results from minimizations using two different values on the weighting parameter is presented. In the first case, in which time is prioritized, the value used is $\beta = 0.01$ and in the second case, in which fuel is prioritized, the value used is $\beta = 0.001$. The resulting time and fuel usages are presented in Table 1. The table shows that by adjusting the weighting parameter the solution can be pushed toward low time or low fuel. The $\beta = 0.01$ fuel consumption resemble values achieved in Nilsson et al. (2012a) while the time needed is lower. In the $\beta = 0.001$ solution on the other hand, the time resemble those of the same paper, but the fuel used is lower.

Table 1. Minimized time and fuel at different values on the weighting parameter β .

β	0.01	0.001
Time [s]	19.7	23.8
Fuel [g]/([ml])	114/(158)	102/(141)

The state trajectories, as functions of distance driven, from the two optimizations are presented in Figures 5 and 6, for $\beta = 0.01$ and $\beta = 0.001$ respectively. The states are vehicle speed v_s , engine speed ω_e and intake air pressure p_t . Along with the intake air pressure, the setpoint pressure p_{set} is presented. The trajectories are similar but in general the levels in all states are higher in the $\beta = 0.01$ solution.

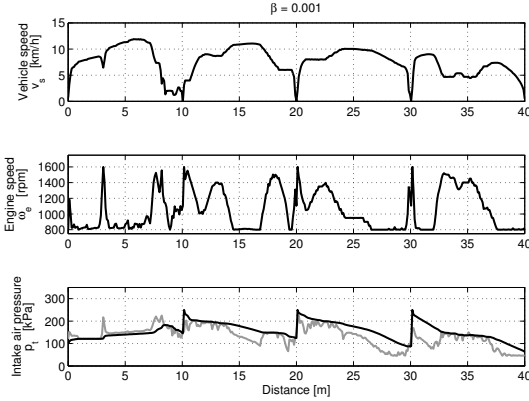


Fig. 5. State trajectories for $\beta = 0.001$.

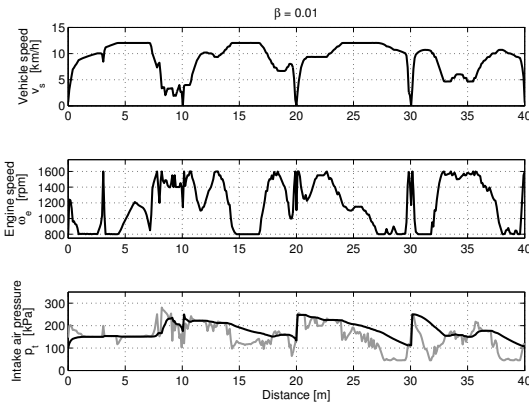


Fig. 6. State trajectories for $\beta = 0.01$.

The control signal trajectories, as functions of distance driven, from the two optimizations are presented in Figures 7 and 8, for $\beta = 0.01$ and $\beta = 0.001$ respectively. The control signals are fuel mass per injection m_f , variator mode m_T , variator displacement ratio ψ_1 and brake torque T_b . Comparing the solutions for the two values of β shows that the gear ratios, composed of the transmission mode m_T and variator ratio ψ_1 , are in general quite similar. In the $\beta = 0.01$ solution the gear ratio is somewhat higher, giving higher vehicle speed for the same engine speed. This means that for the most part the same variator mode is used, and when there is a difference the mode is in general higher in the $\beta = 0.01$ solution. The difference in variator ratio is caused by the different vehicle speeds and the minimum engine speed, as can be seen e.g. at $s = 15m$ in Figures 5 and 6. In the $\beta = 0.001$ solution the vehicle never uses the brakes, but instead reduces the fuel injection early

while in the $\beta = 0.01$ solution the vehicle runs in traction longer and then brakes.

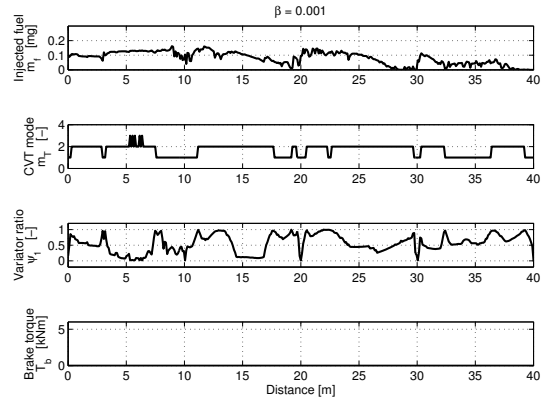


Fig. 7. Control signal trajectories for $\beta = 0.001$.

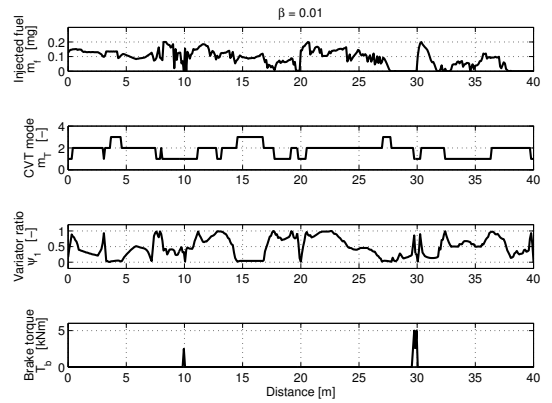


Fig. 8. Control signal trajectories for $\beta = 0.01$.

Figure 9 shows the vehicle speed trajectories from both minimizations, plotted against the time. This figure shows that the difference in time used in the two solutions is evenly spread out between the four driving phases of the cycle. The biggest difference is that the speed near the end of the cycle is noticeable higher in the $\beta = 0.01$ solution.

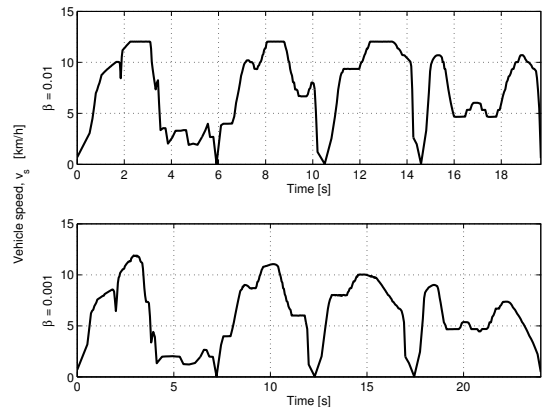


Fig. 9. Vehicle speed trajectories as functions of time for $\beta = 0.01$ and $\beta = 0.001$.

The sensitivity to errors in the predicted bucket load is evaluated by simulating the system with one fix load using $J(k, x)$ maps calculated at different loads. The

vehicle weight was $m_v = 26000\text{kg}$ and the bucket load in the simulation was $m_L = 10000\text{kg}$. The weighting parameter $\beta = 0.001$ is used. The result is summarized in Table 2. For predicted loads lower than the actual, the fuel consumption increase somewhat but for predicted loads higher than the actual, the impact on fuel consumption is negligible. This indicates that the optimization is not highly sensitive to bucket load prediction errors.

Table 2. Fuel and time at varying m_L predictions.

m_L [kg]	fuel [g]/([ml])	time [s]
4000	102.8/(142.8)	24.0
6000	102.6/(142.6)	24.0
8000	101.6/(141.2)	24.2
10000	101.1/(140.5)	24.0
12000	101.2/(140.6)	24.0
14000	101.1/(140.5)	24.0

5. SUMMARY AND CONCLUSIONS

A method is developed for the minimization of time and fuel required for performing a short loading cycle with a wheel loader. A factor β is used for weighing time to fuel in the optimization. Dynamic programming is used as optimization algorithm, and the developed method is based on the change of independent variable, from time to distance driven. With this change of independent variable, the time does not need to be included as a state, thus greatly reducing the computational complexity. It is shown that in the dynamic programming simulations a change of states from speeds to kinetic energies is essential for not introducing simulation errors that give free energy.

A driving cycle, derived from measurements, representing a short loading cycle in the form of driving direction, longitudinal force, hydraulic volume and hydraulic pressure, as functions of distance driven, is introduced. Optimization is performed against this cycle according to the method presented, using different values on the time to fuel weighing parameter. It is shown that this parameter can be used to find solutions directed toward short time or low fuel consumption. The results resemble those presented in Nilsson et al. (2012a), but with either lower time or fuel consumption for completing a loading cycle. Finally, it is shown through an example that the solution is not overly sensitive to uncertainties in the bucket load prediction.

REFERENCES

- Bellman, R. (1957). *Dynamic Programming*. Princeton University Press.
- Bertsekas, D. (2005). *Dynamic Programming and Optimal Control*, volume 1. Athena Scientific, 3 edition.
- Carl, B., Iivantsynova, M., and Williams, K. (2006). Comparison of operational characteristics in power split continuously variable transmissions. In *Commercial Vehicle Engineering Congress and Exhibition*, 2006–01–3468. SAE.
- Filla, R. (2005). An event driven operator model for dynamic simulation of construction machinery. In *Proceedings from the Ninth Scandinavian International Conference on Fluid Power*. Linköping University.
- Filla, R. (2008). Alternative systems solutions for wheel loaders and other construction equipment. In *1st International CTI Forum Alternative and Hybrid Drive Trains*. CTI.
- Grammatico, S., Balluchi, A., and Cosoli, E. (2010). A series-parallel hybrid electric powertrain for industrial vehicles. In *2010 IEEE Vehicle Power and Propulsion Conference*, 1–6. IEEE.
- Hellström, E. (2010). *Look-ahead Control of Heavy Vehicles*. Ph.D. thesis, Linköping University.
- Hellström, E., Åslund, J., and Nielsen, L. (2010). Design of an efficient algorithm for fuel-optimal look-ahead control. *Control Engineering Practice*, 18(11), 1318–1327.
- Lauinger, C., Englisch, A., Gotz, A., Teubert, A., Muller, E., and Baumgartner, A. (2007). Cvt components for powersplit commercial vehicle transmissions. In *Proceedings of the 6th International CTI Symposium*. CTI.
- Lennevi, J. (1995). *Hydrostatic Transmission Control, Design Methodology for Vehicular Drivetrain Applications*. Ph.D. thesis, Linköping University.
- Mattsson, P. and Åkerblom, M. (2012). Continuously variable transmission and a working machine including a continuously variable transmission. Patent. WO 2012/008884 A1.
- Murgovski, N. (2012). *Optimal Powertrain Dimensioning and Potential Assessment of Hybrid Electric Vehicles*. Ph.D. thesis, Chalmers University of Technology.
- Nilsson, T., Fröberg, A., and Åslund, J. (2011). Optimized engine transients. In *7th IEEE Vehicle Power and Propulsion Conference*, 1–6. IEEE.
- Nilsson, T., Fröberg, A., and Åslund, J. (2012a). Fuel potential and prediction sensitivity of a power-split cvt in a wheel loader. In *IFAC Workshop on Engine and Powertrain Control, Simulation and Modeling*, 49–56. IFAC.
- Nilsson, T., Fröberg, A., and Åslund, J. (2012b). Optimal operation of a turbocharged diesel engine during transients. *SAE International Journal of Engines*, 5(2), 571–578.
- Pfiffner, R. and Guzzella, L. (2001). Optimal operation of cvt-based powertrains. *International Journal of Robust and Nonlinear Control*, 11(11), 1003–1021.
- Rizzoni, G., Guzzella, L., and Baumann, B. (1999). Unified modeling of hybrid electric vehicle drivetrains. *IEEE/ASME Transactions on Mechatronics*, 4, 246–257.
- Rydberg, K.E. (1998). Hydrostatic drives in heavy mobile machinery - new concepts and development trends. In *International Off-Highway & Powerplant Congress & Exposition*, 981989. SAE.
- Savaresi, S., Taroni, F., Previdi, F., and Bittanti, S. (2004). Control system design on a power-split cvt for high-power agricultural tractors. *IEEE/ASME Transactions on Mechatronics*, 9(3), 569–579.
- Sivertsson, M. and Eriksson, L. (2012). Optimal short driving mission control for a diesel-electric powertrain. In *8th IEEE Vehicle Power and Propulsion Conference*, 413–418. IEEE.
- Zhang, R. (2002). *Multivariable Robust Control of Nonlinear Systems with Application to an Electro-Hydraulic Powertrain*. Ph.D. thesis, University of Illinois.